



Published in final edited form as:

*Cancer Cell*. 2015 July 13; 28(1): 15–28. doi:10.1016/j.ccell.2015.06.006.

## CHZ868, a Type II JAK2 Inhibitor, Reverses Type I JAK Inhibitor Persistence and Demonstrates Efficacy in Myeloproliferative Neoplasms

Sara C. Meyer<sup>1</sup>, Matthew D. Keller<sup>1</sup>, Sophia Chiu<sup>1</sup>, Priya Koppikar<sup>1</sup>, Olga A. Guryanova<sup>1</sup>, Franck Rapaport<sup>1</sup>, Ke Xu<sup>2</sup>, Katia Manova<sup>2</sup>, Dmitry Pankov<sup>3</sup>, Richard J. O'Reilly<sup>3</sup>, Maria Kleppe<sup>1</sup>, Anna Sophia McKenney<sup>1</sup>, Alan H. Shih<sup>1</sup>, Kaitlyn Shank<sup>1</sup>, Jihae Ahn<sup>1</sup>, Eftymia Papalexi<sup>1</sup>, Barbara Spitzer<sup>1</sup>, Nick Socci<sup>4</sup>, Agnes Viale<sup>4</sup>, Emeline Mandon<sup>5</sup>, Nicolas Ebel<sup>5</sup>, Rita Andraos<sup>5</sup>, Joëlle Rubert<sup>5</sup>, Ernesta Dammassa<sup>5</sup>, Vincent Romanet<sup>5</sup>, Arno Dölemeyer<sup>5</sup>, Michael Zender<sup>5</sup>, Melanie Heinlein<sup>5</sup>, Rajit Rampal<sup>1,9</sup>, Rona Singer Weinberg<sup>7</sup>, Ron Hoffman<sup>8</sup>, William R. Sellers<sup>9</sup>, Francesco Hofmann<sup>5</sup>, Masato Murakami<sup>5</sup>, Fabienne Baffert<sup>5</sup>, Christoph Gaul<sup>5</sup>, Thomas Radimerski<sup>5</sup>, and Ross L. Levine<sup>1,9</sup>

<sup>1</sup>Human Oncology and Pathogenesis Program, Memorial Sloan Kettering Cancer Center, New York, NY

<sup>2</sup>Molecular Cytology, Memorial Sloan Kettering Cancer Center, New York, NY

<sup>3</sup>Department of Pediatrics, Memorial Sloan Kettering Cancer Center, New York, NY

<sup>4</sup>Center for Molecular Oncology, Memorial Sloan Kettering Cancer Center, New York, NY

<sup>5</sup>Novartis Institutes for Biomedical Research, Basel, Switzerland

<sup>6</sup>New York Blood Center, New York, NY

<sup>7</sup>Department of Medicine, Mount Sinai Hospital, New York, NY

<sup>8</sup>Novartis Institutes for Biomedical Research Cambridge, MA

<sup>9</sup>Leukemia Service, Department of Medicine, Memorial Sloan Kettering Cancer Center, New York, NY

### Summary

Although clinically tested JAK inhibitors reduce splenomegaly and systemic symptoms, molecular responses are not observed in most myeloproliferative neoplasms (MPN) patients. We previously demonstrated that MPN cells become persistent to type I JAK inhibitors that bind the active

---

Contact: Ross L. Levine, MD, Human Oncology and Pathogenesis Program, Leukemia Service, Department of Medicine, Memorial Sloan Kettering Cancer Center, 1275 York Ave, Box 20, New York, NY 10065, Phone: 646-888-2767, Fax: 646-422-0856, leviner@mskcc.org; Thomas Radimerski, PhD, Disease Area Oncology, Novartis Institutes for Biomedical Research, Klybeckstrasse 141, 4057 Basel, Switzerland, Phone: 41-61-696-20-64, Fax: 41-61-696-55-11, thomas.radimerski@novartis.com.

**Publisher's Disclaimer:** This is a PDF file of an unedited manuscript that has been accepted for publication. As a service to our customers we are providing this early version of the manuscript. The manuscript will undergo copyediting, typesetting, and review of the resulting proof before it is published in its final citable form. Please note that during the production process errors may be discovered which could affect the content, and all legal disclaimers that apply to the journal pertain.

**Accession number.** RNA sequencing data have been deposited in GEO under accession number GSE69827.

### Author contributions

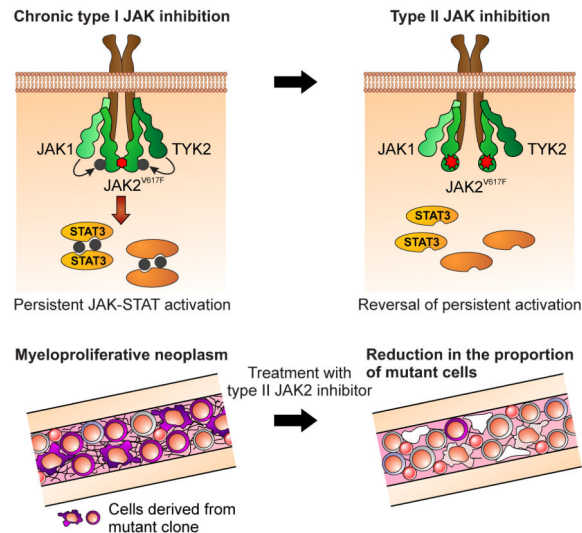
SCM, PK, FB, MM, TR and RLL designed experiments and interpreted results. SCM and RLL wrote and edited the manuscript. SCM, MDK, SC, PK, FR, DP, RO, XK, KM, AHS, KS, BS, NS, AV, EM, NE, RA, JR, ED, VR, AD, MZ, MH, MM, FB, and TR performed experiments. OAG, MK, ASM, RR, RSW, RH contributed murine models or patient samples. CG, MZ, WRS, FH and TR developed CHZ868.

### Disclosure of conflicts of interest

EM, NE, RA, JR, ED, VR, AD, WRS, FH, MM, FB, CG and TR are employees of Novartis Pharma AG. RLL has received research support from Novartis. There are no additional conflicts of interest.

conformation of JAK2. We investigated if CHZ868, a type II JAK inhibitor, would demonstrate activity in JAK inhibitor persistent cells, murine MPN models, and MPN patient samples. *JAK2*- and *MPL*-mutant cell lines were sensitive to CHZ868, including type I JAK inhibitor persistent cells. CHZ868 showed significant activity in murine MPN models and induced reductions in mutant allele burden not observed with type I JAK inhibitors. These data demonstrate that type II JAK inhibition is a viable therapeutic approach for MPN patients.

## Abstract



## Introduction

Myeloproliferative neoplasms (MPN) are myeloid malignancies which present as clonal expansion of one or more myeloid lineages (Dameshek, 1951). The most common MPN are polycythemia vera (PV), essential thrombocythosis (ET), and primary myelofibrosis (PMF). These MPN are characterized by an increased risk of thrombosis and bleeding, transformation to acute leukemia, and bone marrow fibrosis. Mutational studies identified somatic *JAK2*V617F mutations in ~95% of PV and ~50-60% of ET/PMF cases (Baxter et al., 2005; James et al., 2005; Kralovics et al., 2005; Levine et al., 2005; Zhao et al., 2005). Subsequent studies identified *JAK2* exon 12 mutations in *JAK2*V617F-negative PV (Scott et al., 2007), *MPL* (thrombopoietin receptor) mutations in *JAK2*V617F-negative ET/PMF cases (Beer et al., 2008; Pardanani et al., 2006; Pikman et al., 2006; Vannucchi et al., 2008), and *CALR* mutations in *JAK2*/*MPL* wild-type ET/PMF cases (Klampfl et al., 2013; Nangalia et al., 2013).

These discoveries, underscored by recent studies showing that activated JAK-STAT signaling is a characteristic feature of MPN (Rampal et al., 2014), have led to the clinical development of JAK kinase inhibitors in these diseases. In 2011 the JAK1/JAK2 inhibitor ruxolitinib was approved for PMF and post-PV/ET myelofibrosis (MF). Therapy with ruxolitinib and other JAK kinase inhibitors ameliorates splenomegaly and constitutional symptoms in MF patients (Harrison et al., 2012; Verstovsek et al., 2012) and longer term

follow-up suggests ruxolitinib therapy is associated with improved survival compared to placebo or best available therapy (Cervantes et al., 2013; Verstovsek et al., 2013).

Despite these clinical benefits, chronic therapy with JAK inhibitors has not led to molecular or pathologic remissions in the majority of MPN patients (Harrison et al., 2012; Verstovsek et al., 2012) in contrast to ABL kinase inhibitors in chronic myeloid leukemia. The observation that MPN patients do not acquire second-site resistance mutations in *JAK2* during JAK inhibitor therapy suggested MPN cells are able to survive JAK kinase inhibition in the absence of clonal evolution. We recently demonstrated that MPN cells can acquire an adaptive form of resistance, which we termed persistence, to JAK inhibitors through reactivation of JAK-STAT signaling via heterodimerization and trans-activation of JAK2 by JAK1 and TYK2 (Koppikar et al., 2012). shRNA and genetic studies demonstrate that MPN cells remain highly dependent on JAK2 even after in vivo treatment with JAK inhibitors, suggesting approaches which better inhibit JAK2 kinase activity might offer increased therapeutic efficacy (Bhagwat et al., 2014).

Current JAK2 inhibitors in clinical development are type I kinase inhibitors, which stabilize the active kinase conformation. A recent study reported that BBT594, a type II kinase inhibitor originally devised to inhibit the T315I BCR-ABL resistance allele, was able to inhibit JAK2 activity in vitro. BBT594 binds JAK2 in the inactive conformation (“DFG-out” state), where the inhibitor occupies the ATP binding site and an induced hydrophobic pocket (Andraos et al., 2012). The inactive conformation was stabilized consistent with decreased phosphorylation of the activation loop. However, BBT594 has limitations in potency and in selectivity for JAK2, and does not have pharmacokinetic properties for in vivo use. Thus, there is a need to develop type II JAK2 inhibitors with improved potency, selectivity and pharmacokinetics. Here, we investigate the activity of CHZ868, a type II JAK2 inhibitor, in JAK inhibitor persistent cells, preclinical MPN models, and patient samples as an additional approach to therapeutic targeting of JAK2.

## Results

### A common mechanism of persistence to type I JAK inhibitors

Upon prolonged exposure to ruxolitinib, MPN cells become insensitive by acquiring a persistence phenotype with reactivation of JAK-STAT signaling (Koppikar et al., 2012). We investigated whether a similar mechanism of drug persistence would be observed with the type I JAK inhibitors CYT387, BMS911543, and SAR302503. We cultured *JAK2V617F* SET2 cells and *MPLW515L* expressing 32D and TF-1 cells in the presence of different JAK inhibitors for 8-10 weeks. Upon chronic exposure to CYT387, BMS911543 and SAR302503, *JAK2V617F*- and *MPLW515L*-mutant MPN cells acquired a persistence phenotype with a 5- to 30-fold increase in IC<sub>50</sub> to each drug compared to naïve cells (Figure 1A, Figures S1A-D). CYT387, BMS911543 and SAR302503 did not inhibit STAT3, STAT5, or ERK1/2 phosphorylation in persistent cells (Figure S1E), consistent with a lack of target inhibition. Gene set enrichment analysis demonstrated significant enrichment of an activated STAT5 gene expression signature (Schuringa et al., 2004) in persistent cells (Figure 1B, Figure S1F). We also observed reduced expression of apoptosis gene expression signatures, consistent with the increased survival of persistent cells (Figure 1C; Figure S1G).

Principal component analysis (PCA) of RNA-sequencing data separated type I JAK inhibitor persistent cells from naive cells based on differential gene expression (Figure S1H-I). We did not identify acquired mutations in *JAK2*, *JAK1*, or *TYK2* in any of the persistent lines, and persistence to CYT387, BMS911543 and SAR302503 was reversible after drug withdrawal (data not shown).

We next investigated whether activated JAK2 interacted with JAK1 or TYK2 in CYT387, BMS911543 and SAR302503 persistent cells, as shown previously for ruxolitinib persistence (Koppikar et al., 2012). We observed increased association of phosphorylated JAK2 and JAK1/TYK2 in JAK inhibitor persistent cells (Figure S1J), and heterodimer formation increased over time (Figure S1K). Immunofluorescence confirmed heterodimers were localized near the plasma membrane in CYT387 and ruxolitinib persistent cells (Figure S1L), and we observed JAK1-JAK2 co-localization in persistent cells (Figures S1M-N). MPN cells which acquired persistence to a specific type I JAK inhibitor were cross-persistent to all other type I JAK inhibitors (Table 1, Figure 1D). These data demonstrate that type I JAK inhibitors in clinical development cannot overcome persistence induced by another type I inhibitor.

### **Type II Inhibition with CHZ868 demonstrates efficacy in *JAK2* and *MPL* mutant MPN cells**

A previous study reported that BBT594, a type II kinase inhibitor designed to inhibit the BCR-ABL T315I resistance allele, had significant activity in JAK-dependent cellular assays (Andraos et al., 2012). However, this agent was limited in potency, specificity and pharmacokinetic properties for in vivo assessments. Our drug discovery efforts focusing on chemical scaffolds known to stabilize kinases in their inactive (type II) conformation led to the discovery of a benzimidazole analogue, CHZ868 (cf. accompanying submission by Wu S-C et al). CHZ868 potently inhibited constitutive JAK2 and STAT5 phosphorylation in *JAK2V617F* SET2 cells (Figure S1O), whereas 5- to 10-fold higher CHZ868 concentrations were required to suppress constitutive JAK3 and STAT5 phosphorylation in *JAK3A572V* mutant CMK cells (Figure S1P). Consistent with the notion that CHZ868 has a bias to inhibit JAK2 over JAK3, CHZ868 potently inhibited the proliferation of SET2 cells ( $GI_{50}=59\text{nM}$ ), and had 6-fold less growth inhibitory activity against CMK cells ( $GI_{50}=378\text{nM}$ ). In contrast to BBT594, CHZ868 lacked activity against BCR-ABL as demonstrated by insensitivity of K562 cells ( $GI_{50}=4627\text{nM}$ ) (Figure S1Q). To assess cellular activity against JAK1 and TYK2, we first assessed the impact of CHZ868 on nuclear translocation of STAT1 upon stimulation of TF-1 cells with  $\text{INF-}\alpha$ . We observed a 60- to 70-fold higher  $IC_{50}$  for inhibition of JAK1-/TYK2-mediated nuclear STAT1 translocation by CHZ868 compared to pan-JAK inhibitor tofacitinib (Figures S1R-S). CHZ868 suppressed JAK1 and TYK2 signaling in  $\text{INF-}\alpha$  stimulated TF-1 cells at 10-fold higher concentrations than JAK2 signaling in SET2 cells (Figure S1T). Moreover, CHZ868 showed less potent ability to inhibit the proliferation of isogenic Ba/F3 cells stably expressing constitutively active JAK1 V658F and TYK2 V678F compared to cells expressing JAK2 V617F; we observe growth inhibition at 4-fold and 24-fold higher  $IC_{50}$  values, respectively, as compared to JAK2 V617F (Figure 1E). These results demonstrate that CHZ868 most potently inhibits JAK2 among the JAK kinases.

Next, we assessed the activity of CHZ868 to *MPL* mutant cells in vitro. As in SET2 cells, CHZ868 potently inhibited the proliferation of 32D cells expressing *MPLW515L* (Figures 1F-G). CHZ868 treatment abrogated phosphorylation of Y1007/Y1008 in the JAK2 activation loop, consistent with a type II mechanism of action (Figure 1H, Figure S1O). By contrast, ruxolitinib exposure led to JAK2 stabilization and persistent activation loop phosphorylation (Figure 1H) (Andraos et al., 2012). Inhibitor washout studies confirmed that phosphorylation of JAK2 and STAT5 was gradually restored within 4-24 hr after removing CHZ868 (Figure S1U). CHZ868 potently induced apoptosis in *JAK2* and *MPL* mutant cells as reflected by caspase 3 activation (Figure 1I) and by annexin V staining (Figure S1V), and exhibited enhanced killing of *JAK2V617F* SET2 cells compared to ruxolitinib. These findings demonstrate that type II JAK2 inhibition with CHZ868 shows significant activity in *JAK2V617F* and *MPLW515L* mutant cells, including potent inhibition of JAK2 and STAT phosphorylation and induction of cell death.

We further investigated the sensitivity of mutant vs. wild-type JAK2 to CHZ868 in Ba/F3 cells stably expressing JAK2 V617F or JAK2 WT co-expressed with the erythropoietin receptor (EPOR), using EPO to activate EPOR/JAK2 signaling in WT cells. CHZ868 suppressed the phosphorylation of STAT3 and STAT5 at 2- to 3-fold lower concentrations in JAK2 V617F than in JAK2 WT cells (Figures 1J-K). Concordant with effects on signaling, CHZ868 more potently inhibited the proliferation of JAK2 V617F cells, with  $IC_{50}$  values 2- to 3-fold lower than the growth of JAK2 WT cells ( $IC_{50}$  JAK2 V617F 0.06  $\mu$ M, JAK2 WT 0.17  $\mu$ M, Figure 1L). In contrast, we saw equivalent growth inhibitory activity of ruxolitinib in JAK2 V617F and WT cells (Figure 1M). These findings demonstrate that type II JAK2 inhibition with CHZ868 shows increased relative activity against JAK2 V617F vs. JAK2 WT cells (Figure 1N).

### **Type II JAK inhibition by CHZ868 overcomes persistence to type I JAK inhibitors**

We next investigated whether CHZ868 could inhibit JAK-STAT signaling and attenuate proliferation of type I JAK inhibitor-persistent cells. CHZ868 exposure led to potent, concentration-dependent inhibition of JAK2 phosphorylation in CYT387, BMS911543, and ruxolitinib persistent cells (Figure 2A). CHZ868 treatment abrogated STAT3 and STAT5 phosphorylation in persistent cells, whereas type I JAK inhibitors had no effect on signaling. Concordant with the signaling data, CHZ868 exposure led to concentration-dependent inhibition of proliferation of *JAK2V617F* or *MPLW515L* cells that were insensitive to CYT387, SAR302503, BMS911543 and ruxolitinib (Figure 2B, Figure S2). The  $IC_{50}$  to CHZ868 was 5- to 16-fold lower compared to the  $IC_{50}$  for type I inhibitors in persistent SET2 or 32D *MPLW515L* cells, and was similar to the  $IC_{50}$  observed in inhibitor naïve cells (Figure 2C). CHZ868 exposure led to a concentration-dependent increase in apoptosis in ruxolitinib (Figure 2D), BMS911543 (Figure 2E) and CYT387 (not shown) persistent cells, whereas exposure of persistent cells to type I inhibitors did not induce significant apoptosis.

To elucidate the mechanism by which CHZ868 reverses inhibitor persistence, we performed co-immunoprecipitation studies with JAK1 or TYK2 followed by Western blot analysis of JAK2 phosphorylation at the Y1007/Y1008 tandem tyrosine in the activation loop. Consistent with the Western blot studies for phosphorylated JAK2, we did not observe any



phosphorylated JAK2 bound to JAK1 or TYK2 in persistent cells cultured in the presence of CHZ868 (Figure 3A). The loss of activated JAK2 bound to JAK1 and TYK2 was sustained, with complete absence of JAK2 activation loop phosphorylation after 20 hr of CHZ868 exposure, suggesting type II inhibition durably abolishes JAK2 activation (Figure 3B). As CHZ868 did not inhibit dimerization between unphosphorylated JAK2 and JAK1/TYK2, we investigated how CHZ868 interfered with transphosphorylation of JAK2 by JAK1/TYK2 in heterodimers. Given the bias of CHZ868 towards inhibition of JAK2 over JAK1 and TYK2 (Figure 1E), we hypothesized that type II inhibition restricted accessibility of JAK2 for transphosphorylation by stabilizing JAK2 in the inactive form. We expressed constitutively active JAK1 V658F and kinase-dead JAK2 K882E in  $\gamma$ 2A cells deficient of endogenous JAK2, such that all JAK2 activation occurs in trans by activated JAK1. CHZ868 abrogated JAK1-mediated Y1007/Y1008 phosphorylation of JAK2 K882E at concentrations which did not fully inhibit JAK1 autophosphorylation (Figure 3C). This finding demonstrated that type II inhibition by CHZ868 attenuates JAK2 transphosphorylation in heterodimers by inhibiting JAK1 activity and by restricting accessibility of JAK2 for transphosphorylation at the activation loop.

We next evaluated the impact of CHZ868 on other phosphorylation sites known to be involved in the regulation of JAK2 kinase activity. We assessed the ability of CHZ868 to impact JAK1-mediated phosphorylation of Y221, which has a known activating role for JAK2 (Argetsinger et al., 2004). Concordant with suppressed phosphorylation at Y1007/1008, CHZ868 inhibited phosphorylation at Y221 in type I JAK inhibitor persistent cells (Figure 3D, top row). By contrast, CHZ868 did not alter the phosphorylation of Y570 and S523, which are implicated in negative regulation of JAK2 activity (Argetsinger et al., 2004; Bandaranayake et al., 2012; Ungureanu et al., 2011) (Figure 3D, middle and bottom row). These findings suggest that type II JAK inhibition with CHZ868 renders activating phospho-sites of JAK2 not (Y1007/1008) or less (Y221) accessible for transphosphorylation in heterodimers, whereas phosphorylation of inhibitory sites in the JH2 domain remains intact, which overall results in inhibition of JAK2 activity and suppression of JAK-STAT signaling in type I inhibitor persistent cells.

To investigate the impact of CHZ868 on type I inhibitor persistence in vivo, we treated C3H/HeJ mice engrafted with Rux<sup>Per</sup> 32D *MPLW515L* cells (Figure S3A-B). Vehicle-treated animals succumbed to disease within 20 days of transplantation with splenomegaly (Figure S3C-D) and hepatomegaly (Figure S3E), infiltration of bone marrow (Figure S3B), lung and liver (Figure S3F-G). Treatment with CHZ868 at 40 mg/kg once daily normalized splenomegaly within 7 days of treatment (Figure S3C-D), and reduced leukemic infiltration of lung and liver (Figure S3F-G). CHZ868 significantly prolonged survival of C3H/HeJ mice transplanted with Rux<sup>Per</sup> 32D *MPLW515L* cells (Figure S3H).

We next assessed the effect of CHZ868 on inhibition of JAK2 signaling in primary samples from ruxolitinib treated MF patients. In line with previous reports (Bhagwat et al., 2014; Koppikar et al., 2012), we observed pronounced activation of STAT3 and STAT5 in peripheral blood mononuclear cells from MF patients receiving chronic ruxolitinib therapy. By contrast, CHZ868 completely suppressed phosphorylation of STAT3 and STAT5 (Figure 3E). We observed dose-dependent inhibition of pSTAT3 and pSTAT5 with strong inhibitory

effects at low concentrations (Figure 3F). These data demonstrate CHZ868 inhibits JAK-STAT signaling in MPN patient cells which persist during chronic ruxolitinib treatment.

### CHZ868 shows significant efficacy in *Jak2V617F*-driven polycythemia vera

We next assessed the efficacy of CHZ868 at inhibiting myeloproliferation in vivo. We first used *Jak2V617F* conditional knock-in mice (Mullally et al., 2010) crossed with a Vav-cre allele to express *Jak2V617F* in the hematopoietic compartment. We transplanted CD45.2 *Jak2V617F* and CD45.1 *Jak2* WT cells into CD45.1 recipients to allow us to assess the impact of CHZ868 on the mutant clone in vivo compared to wild-type cells. CHZ868 dosed at 30-40 mg/kg orally once daily inhibited JAK-STAT signaling in vivo consistent with potent target inhibition (Figure 4A). CHZ868 therapy resulted in significant reduction in the proportion of mutant cells in the bone marrow (Figure 4B). We also observed a significant decrease of mutant allele burden in the CD71<sup>+</sup>Ter119<sup>+</sup> erythroid progenitor compartment with CHZ868 as compared to vehicle-treated mice (Figure 4C), consistent with a mutant-biased reduction in erythroid output. These data demonstrate that type II JAK2 inhibition with CHZ868 reduces mutant allele burden in vivo, which we and others have not observed with type I inhibitors in preclinical models (Kubovcakova et al., 2013; Mullally et al., 2010; Tyner et al., 2010).

Consistent with the effects on disease burden, CHZ868 normalized spleen and liver weights, demonstrating marked inhibition of extramedullary hematopoiesis (Figure 4D). Peripheral blood count analysis showed that CHZ868 reduced hematocrit from 71% in vehicle-treated mice to 51.1% and 49.4% with 30 and 40 mg/kg CHZ868, respectively (Figure 4E). CHZ868 therapy normalized the modestly elevated white blood cell count seen in the *Jak2V617F* model of PV. Histopathologic analysis demonstrated CHZ868 therapy restored normal splenic architecture, in contrast to the myelo-erythroid infiltration observed in vehicle-treated animals (Figure 4F). CHZ868 therapy reduced the bone marrow megakaryocytic hyperplasia seen in vehicle-treated mice (Figure 4G). The expansion of erythroid progenitors characteristic of *Jak2V617F* knock-in bone marrow was significantly reduced with CHZ868 therapy. We observed significantly reduced erythroid progenitors with type II Jak2 inhibition, including CD71<sup>+</sup>Ter119<sup>+</sup> proerythroblasts (Figure 4H,  $p=0.036$  and  $p=0.015$ ), Lin<sup>-</sup>cKit<sup>high</sup>CD41<sup>-</sup>FcγR<sup>-</sup>CD150<sup>+</sup>CD105<sup>+</sup> Pre-CFUE ( $p<0.01$  and  $p<0.001$ ) and Lin<sup>-</sup>cKit<sup>high</sup>CD41<sup>-</sup>FcγR<sup>-</sup>CD150<sup>+</sup>CD105<sup>-</sup> Pre-MegE ( $p=0.02$  and  $p<0.01$ ) as described (Pronk et al., 2007) (Figures 4I, J). CHZ868 also decreased the proportion of myelo-erythroid progenitors, including Lin<sup>-</sup>Sca1<sup>-</sup>Kit<sup>+</sup> multipotent myeloid progenitors (Figures 4J, K,  $p=0.02$ ).

We performed additional studies in a second model of PV-like disease, in which mice were engrafted with bone marrow retrovirally transduced with *Jak2V617F*-IRES-GFP. Consistent with the efficacy of CHZ868 in the *Jak2V617F* conditional knock-in model, CHZ868 at 30 mg/kg orally once daily completely reverted splenomegaly and reduced hematocrit, reticulocyte and WBC counts (Figures S4A-D). We observed a significant reduction in mutant allele burden with CHZ868 therapy also in the retroviral *Jak2V617F* transplant model, as reflected by a reduction in the proportion of circulating GFP<sup>+</sup> cells (Figure S4E). Consistent with the effect on disease burden, CHZ868 therapy inhibited phosphorylated

STAT5 as assessed by IHC in spleen and bone marrow (Figures S4F-G). Furthermore, histopathology assessment revealed that CHZ868 therapy resulted in decreased splenic erythro- and myeloproliferation, decreased bone marrow hypercellularity (Figure S4H, top and middle) and in a reduction of reticulin fiber deposits (Figures S4H-I).

### Efficacy of CHZ868 in *MPLW515L*-induced myelofibrosis

We next assessed the efficacy of CHZ868 in a murine model of PMF-like disease. We used the retroviral bone marrow transplant (BMT) model of *MPLW515L*-induced MF, which leads to a fully penetrant, lethal MPN characterized by severe myelofibrosis (Koppikar et al., 2010). CHZ868 completely suppressed STAT5 and STAT3 phosphorylation (Figure 5A). JAK2 phosphorylation was also reduced, consistent with the type II binding mode of CHZ868. CHZ868-mediated inhibition of JAK-STAT signaling was maintained with 10 days of treatment consistent with chronic, potent target inhibition (data not shown). CHZ868 therapy significantly improved survival of mice with *MPLW515L*-induced myelofibrosis (Figure 5B,  $p < 0.0001$ , 10-11 mice/arm) and resulted in dose-dependent reduction of hepatomegaly (Figure 5C) and normalization of spleen weight and size with 40 mg/kg CHZ868 (Figure 5D). CHZ868 dose-dependently reduced extramedullary hematopoiesis in liver and spleen, with complete restoration of liver/spleen tissue architecture in the 40 mg/kg arm (Figure 5E). CHZ868 reduced bone marrow megakaryocytosis (Figure 5E) and bone marrow and spleen hypercellularity (Figure S5A), features characteristic of *MPLW515L*-induced MF. CHZ868 therapy resulted in dose-dependent reduction in *MPLW515L*-induced leukocytosis ( $p = 0.035$ ) and thrombocytosis ( $p < 0.01$ ), consistent with CHZ868-mediated inhibition of myeloproliferation (Figure 5F). In addition to *MPLW515L*-induced myelofibrosis in Balb/C mice, therapeutic effects of CHZ868 were confirmed in C57BL/6 mice using the *MPLW515L* BMT model (Figures S5B-D) to enable flow cytometric analysis of progenitor populations. CHZ868 therapy resulted in a trend towards reduced proportions of Lin<sup>-</sup>Sca1<sup>-</sup>Kit<sup>+</sup> multipotent myeloid progenitors and Lin<sup>-</sup>Sca1<sup>-</sup>Kit<sup>+</sup>FcγR<sup>-</sup>CD34<sup>-</sup> megakaryocytic-erythroid progenitor populations (Figures 5G-H). Importantly, CHZ868 therapy markedly decreased bone marrow and spleen reticulin fibrosis, consistent with disease-modifying activity (Figure 5I, Figure S5E). In addition, CHZ868 therapy significantly reduced mutant allele burden as reflected by a reduction in the proportion of GFP<sup>+</sup> cells in peripheral blood (Figure 5J,  $p = 0.017$ ).

As we observed significant reductions of mutant allele burden not observed with type I inhibitors in these MPN models, we investigated whether CHZ868 had differential cytotoxic effects on bone marrow hematopoietic progenitors. We used immunofluorescent staining for cleaved caspase-3 in the *MPLW515L* model and flow cytometric analyses of annexin V positivity in the *MPLW515L* and the *Jak2V617F* knock-in models after in vivo treatment with CHZ868. CHZ868 strongly reduced *MPLW515L* GFP<sup>+</sup> megakaryocytes in bone marrow and spleen, and induced apoptosis in vivo (Figure S5F). We observed an increase in *MPLW515L* GFP/cleaved Caspase-3 double-positive cells compared to *MPL* WT GFP<sup>-</sup> megakaryocytes (arrowheads) consistent with increased susceptibility for apoptosis induction by CHZ868 in the mutant compartment. Concordant with this observation, flow cytometric analysis of annexin V positivity showed, that CHZ868 induced increased apoptosis in *MPLW515L* vs. *MPL* WT and in *Jak2V617F* vs. *Jak2* WT Lin<sup>-</sup>Sca1<sup>-</sup>Kit<sup>+</sup>





However, these approaches require investigation of combinations, and may result in increased toxicity due to inhibition of multiple, essential cellular pathways.

We therefore investigated the efficacy of type II JAK2 inhibition with CHZ868, which binds JAK2 in the inactive conformation in contrast to type I inhibitors that bind JAK2 in the active form. CHZ868 had similar efficacy in type I JAK inhibitor naive and persistent cells and a bias towards inhibition of mutant JAK2 V617F over wild-type JAK2, consistent with a different mechanism of JAK kinase inhibition. We observed potent suppression of JAK signaling, proliferation, and induction of apoptosis in MPN cells by CHZ868 regardless of previous exposure to type I JAK inhibitors. These data demonstrate that type I JAK inhibitor persistent cells remain sensitive to type II JAK inhibitors, and that CHZ868 retains therapeutic efficacy in cells which acquire insensitivity to clinically utilized JAK inhibitors. We hypothesized that the mechanism by which type II inhibition abrogates cross-persistence relates to the stabilization of JAK2 in the inactive conformation. This may occur by blocking JAK2 monomers in the inactive state and shifting the equilibrium away from JAK heterodimers which contain the active form of the kinase. Alternatively, type II inhibition might overcome cross-persistence by directly inhibiting JAK2 in the heterodimers. CHZ868 promptly inactivated JAK2 incorporated in JAK heterodimers, and JAK-STAT signaling was simultaneously abrogated without a requirement for heterodimer dissociation. Concordant with a bias towards inhibition of JAK2 over JAK1 and TYK2, CHZ868 suppressed transphosphorylation of kinase-dead JAK2 at the activation loop, suggesting that CHZ868 renders the JAK2 activation loop inaccessible for transphosphorylation. We found a differential interference of CHZ868 with inhibition of activating phosphorylation events at Y1007/1008 and at Y221, and preserved phosphorylation at regulatory sites in the pseudokinase domain at Y570 and S523 resulting in a net, profound inhibition of heterodimeric JAK2. These findings suggest that inactivation of heterodimeric JAK2 by type II inhibition involves differential changes in the accessibility of functionally different phospho-sites interfering with transactivation.

Consistent with the in vitro data, in preclinical models of *Jak2*V617F-induced PV and *MPLW515L*-induced MF, CHZ868 treatment reversed MPN hallmarks, including splenomegaly, pathologic erythrocytosis, thrombocytosis and leukocytosis, and alterations in bone marrow progenitor populations induced by constitutive *Jak2* or *MPL* mutant alleles. CHZ868 therapy attenuated reticulin fibrosis, a key pathologic MF trait that persists with chronic type I JAK inhibitor therapy. Most importantly, CHZ868 therapy induced a significant decrease in mutant allele burden in preclinical models of PV and MF based on an increased susceptibility of *Jak2*V617F and *MPLW515L* cells to CHZ868 in vitro and in vivo. The molecular and histologic responses seen with CHZ868 therapy suggest a disease-modifying effect of type II JAK inhibition in MPN, similar to that observed with CHZ868 in *JAK2*R683G mutated B-ALL models (cf. accompanying manuscript by Wu S-C et al).

Although subsequent preclinical and clinical studies are needed to delineate efficacy and toxicity of type II JAK inhibition, these data suggest that alternate mechanisms of kinase inhibition can increase therapeutic benefit. We anticipate that similar approaches for other mutated kinases might offer similar benefit in other malignant contexts. Most importantly, our data demonstrate that current approaches to target JAK2 have not fully tested the

dependency for JAK2 kinase activity in the clinical contexts, and suggest the need to explore additional approaches to improve target inhibition in the malignant clone, and to improve outcomes for patients with MPNs, as well as with other malignancies characterized by activated JAK2 signaling.

## Experimental Procedures

### Inhibitors

CHZ868 was synthesized by Novartis and stored at 1mM in DMSO for in vitro use. For in vivo applications, CHZ868 was administered orally at 15 mg/kg twice daily (bid) or at 15, 20, 30 or 40 mg/kg once daily (qd). CYT387, BMS911543 and ruxolitinib were purchased from Chemietek. SAR302503 was synthesized as described (Marubayashi et al., 2010); these agents were stored at 1mM in DMSO at -20°C.

### Cell lines

SET2 cells were cultured in RPMI1640/20% FCS. 32D and TF-1 cells were transduced with viral supernatants containing MSCV-*hMPLW515L*-IRES-GFP (Pikman et al., 2006), FACS-sorted for GFP and cultured in RPMI1640/10% FCS. A panel of SET2, 32D *MPLW515L* and TF-1 *MPLW515L* cell lines persistent to CYT387, BMS911543, SAR302503 or ruxolitinib were generated by culture in presence of increasing inhibitor concentrations for 8-10 weeks. Resensitization was induced by drug withdrawal. Ba/F3 cells stably expressing JAK2 V617F/EPOR were cultured in RPMI1640/10%FCS, supplemented with 10U/ml EPO in case of Ba/F3 cells expressing JAK2 WT/EPOR. Ba/F3 cells stably expressing TYK2 V678F (generously provided by S. Constantinescu) or JAK1 V658F were cultured in RPMI1640/10%FCS.  $\gamma$ 2A cells deficient of endogenous JAK2 and stably expressing JAK1 V658F and JAK2 K882E were maintained in DME/10% FCS.

### In vitro inhibitor assays

To assess anti-proliferative effects of inhibitors, all cell lines were cultured at 10,000 cells/200  $\mu$ l with increasing inhibitor concentrations in triplicate. Proliferation was assessed at 48 hr using the Cell viability luminescent assay (Promega) and normalized to cell growth in media with an equivalent volume of DMSO (Koppikar et al., 2010). The concentration inhibiting proliferation by 50% (IC<sub>50</sub>) was determined with Graph Pad Prism 5.0. Anti-proliferative activity of inhibitors in SET2, CMK and K562 cells was also determined by incubation for 72 hr and proliferation measured by colorimetric WST-1 cell viability readout (Roche). Of each triplicate the mean was calculated and data were plotted in XLfit 4 (ID Business Solutions Ltd) to determine half-maximal growth inhibition (GI<sub>50</sub>).

### Transcriptional profiling, gene set enrichment analysis (GSEA) and principal component analysis (PCA)

SET2 cells were treated with ruxolitinib at 0.7  $\mu$ M for 4 hr, left untreated, or, in case of the type I inhibitor persistent SET2 cells, chronically cultured in presence of CYT387, BMS911543, SAR302503 or ruxolitinib. Triplicate samples were lysed in TRIzol (Life Technologies). Please see Supplemental Methods for details on sequencing and expression analysis.

### Induction of apoptosis

Naive or type I JAK inhibitor persistent cells were cultured for 24 hr at  $10^6$  cells/ml with increasing inhibitor concentrations, washed twice in ice-cold PBS and assessed for apoptosis induction by CASPASE-3 MAB APOPTOSIS KIT (BD) or by Annexin V PE apoptosis kit (BD) and flow cytometry on LSRFortessa (BD).

### JAK signaling and heterodimer formation

Cells were incubated at  $10^6$ /ml media with inhibitor or DMSO for 4 hr, washed in ice-cold PBS and collected in lysis buffer with Protease Arrest (G-Biosciences) and Phosphatase Inhibitor Cocktail II (EMD). Ba/F3 EPOR JAK2 WT cells were serum starved overnight prior to inhibitor exposure, and incubated with 2 U/ml EPO and inhibitor for 4 hr. Total protein was normalized by Bio-Rad Bradford quantitation, separated on 4-12% Bis-Tris gels (Invitrogen) and blots probed for pJAK2, JAK2, pSTAT3, STAT3, pSTAT5, Actin (CST) and STAT5 (Santa Cruz). NIH Image J was used for densitometry. JAK heterodimer formation was assessed by immunoprecipitation for JAK1 and TYK2 (BD) followed by detection of pJAK2, pJAK1, JAK2 (CST) and of JAK1 and TYK2 (BD). JAK2 phosphorylation was assessed at Y1007/Y1008 (CST), Y221 (CST), Y570 (Millipore) and S523 (antibody generously provided by O. Silvennoinen). For analysis of in vivo signaling, mice were sacrificed 2 hr after oral CHZ868. Red cell lysed splenocyte single cell suspensions were processed as described above.

### Signaling analysis in patient samples

The institutional review board of Memorial Sloan Kettering Cancer Center approved sample collection and experiments. Informed consent was obtained from all patients providing material for studies. Peripheral blood mononuclear cells were freshly extracted using Ficoll separation and treated ex vivo with increasing concentrations of CHZ868 or DMSO for 16 hr. 50-60  $\mu$ g protein of whole cell lysate was separated on 4-12% Bis-Tris electrophoresis gels and blots were probed for pSTAT3, STAT3, pSTAT5 and Actin (CST) and STAT5 (Santa Cruz).

### Animal models of polycythemia vera and myelofibrosis

For treatment studies in the conditional *Jak2V617F* knock-in model of PV, bone marrow from primary CD45.2 *Jak2V617F* mice (Mullally et al., 2010) was mixed 1:1 with CD45.1 C57BL/6 marrow and transplanted into lethally irradiated CD45.1 C57BL/6 recipients. Mice were randomized to the three groups vehicle, 30 mg/kg or 40 mg/kg CHZ868 qd according to blood counts, and treated by oral gavage for 2-3 weeks. For studies in the *MPLW515L* model of MF, CD117-enriched (Miltenyi) Balb/c marrow was transduced with retroviral supernatant containing MSCV-*hMPLW515L*-IRES-GFP and injected into lethally irradiated Balb/c recipients (Koppikar et al., 2010). Mice were randomized according to blood counts to receive vehicle, 30 mg/kg or 40 mg/kg CHZ868 qd for 10 days-3 weeks. *MPLW515L* transplants in C57BL/6 mice were performed analogously. For pharmacodynamic analyses, *MPLW515L* Balb/c or primary *Jak2V617F* C57BL/6 mice received 1-3 doses of CHZ868 and were sacrificed 2 hr later. For histopathology, tissues were fixed in 4% paraformaldehyde, paraffin-embedded and stained with hematoxylin/eosin. For assessment

of reticulin fibrosis, the silver impregnation kit for reticular fibers (Bio-Optica) was used and reticulin fibrosis was graded according to histology scores. Animal care was in strict compliance with institutional guidelines established by Memorial Sloan Kettering Cancer Center, the Guide for Care and Use of Laboratory animals and the Association for Assessment and Accreditation of Laboratory Animal Care International. All animal procedures were conducted in accordance with the Guidelines for the Care and Use of Laboratory Animals and were approved by the Institutional Animal Care and Use Committees at Memorial Sloan Kettering Cancer Center. For analyses in the *Jak2V617F* BMT model, experiments were performed in strict adherence to Swiss laws for animal welfare, and approved by the Swiss Cantonal Veterinary Office of Basel-Stadt.

### Flow cytometry for erythroid progenitor populations and mutant allele burden

In *Jak2V617F* and *MPLW515L* BMT models, allele burden was determined as percentage of GFP<sup>+</sup> cells in peripheral blood. In competitive transplants of *Jak2V617F* knock-in marrow, allele burden was assessed as fraction of CD45.2 marrow or spleen cells. For analysis of the erythroid progenitor populations, marrow and spleen cells were stained for lineage markers, Sca-1, c-Kit, CD41, CD150, CD48, CD16/32 and CD105, CD71 and Ter119 (eBioscience) as described (Pronk et al., 2007) and analyzed on LSRFortessa or FACS Aria III (BD).

### Supplementary Material

Refer to Web version on PubMed Central for supplementary material.

### Acknowledgements

We thank David Weinstock, Omar Abdel-Wahab and members of the Levine Laboratory for helpful comments on the manuscript, Ann Mullally for *Jak2V617F* mice, Stefan Constantinescu for TYK2 V678F Ba/F3 cells and Olli Silvennoinen for pS523 antibody. This work was supported by NCI 1R01CA151949-01 to RLL, by fellowships of Swiss National Science Foundation, Swiss Cancer League, and Huggenberger-Bischoff Foundation for Cancer Research to SCM, by NIH/NCI 1K99CA178191 to OAG, by NIH T32GM007739/5F30CA183497 to ASM and by research support from Novartis. MK is a Leukemia and Lymphoma Society fellow. RLL is a Leukemia and Lymphoma Society Scholar.

### References

- Alcala S, Klee M, Fernandez J, Fleischer A, Pimentel-Muinos FX. A high-throughput screening for mammalian cell death effectors identifies the mitochondrial phosphate carrier as a regulator of cytochrome c release. *Oncogene*. 2008; 27:44–54. [PubMed: 17621274]
- Andraos R, Qian Z, Bonenfant D, Rubert J, Vangrevelinghe E, Scheufler C, Marque F, Regnier CH, De Pover A, Ryckelynck H, et al. Modulation of activation-loop phosphorylation by JAK inhibitors is binding mode dependent. *Cancer discovery*. 2012; 2:512–523. [PubMed: 22684457]
- Argetsinger LS, Kouadio JL, Steen H, Stensballe A, Jensen ON, Carter-Su C. Autophosphorylation of JAK2 on tyrosines 221 and 570 regulates its activity. *Molecular and cellular biology*. 2004; 24:4955–4967. [PubMed: 15143187]
- Bandaranayake RM, Ungureanu D, Shan Y, Shaw DE, Silvennoinen O, Hubbard SR. Crystal structures of the JAK2 pseudokinase domain and the pathogenic mutant V617F. *Nature structural & molecular biology*. 2012; 19:754–759.
- Baxter EJ, Scott LM, Campbell PJ, East C, Fourouclas N, Swanton S, Vassiliou GS, Bench AJ, Boyd EM, Curtin N, et al. Acquired mutation of the tyrosine kinase JAK2 in human myeloproliferative disorders. *Lancet*. 2005; 365:1054–1061. [PubMed: 15781101]



- Beer PA, Campbell PJ, Scott LM, Bench AJ, Erber WN, Bareford D, Wilkins BS, Reilly JT, Hasselbalch HC, Bowman R, et al. MPL mutations in myeloproliferative disorders: analysis of the PT-1 cohort. *Blood*. 2008; 112:141–149. [PubMed: 18451306]
- Bhagwat N, Koppikar P, Keller M, Marubayashi S, Shank K, Rampal R, Qi J, Kleppe M, Patel HJ, Shah SK, et al. Improved targeting of JAK2 leads to increased therapeutic efficacy in myeloproliferative neoplasms. *Blood*. 2014; 123:2075–2083. [PubMed: 24470592]
- Cervantes F, Vannucchi AM, Kiladjian JJ, Al-Ali HK, Sirulnik A, Stalbovska V, McQuitty M, Hunter DS, Levy RS, Passamonti F, et al. Three-year efficacy, safety, and survival findings from COMFORT-II, a phase 3 study comparing ruxolitinib with best available therapy for myelofibrosis. *Blood*. 2013; 122:4047–4053. [PubMed: 24174625]
- Dameshek W. Some speculations on the myeloproliferative syndromes. *Blood*. 1951; 6:372–375. [PubMed: 14820991]
- Deshpande A, Reddy MM, Schade GO, Ray A, Chowdary TK, Griffin JD, Sattler M. Kinase domain mutations confer resistance to novel inhibitors targeting JAK2V617F in myeloproliferative neoplasms. *Leukemia*. 2012; 26:708–715. [PubMed: 21926964]
- Evrot E, Ebel N, Romanet V, Roelli C, Andraos R, Qian Z, Dolemeyer A, Dammassa E, Sterker D, Cozens R, et al. JAK1/2 and Pan-deacetylase inhibitor combination therapy yields improved efficacy in preclinical mouse models of JAK2V617F-driven disease. *Clinical cancer research: an official journal of the American Association for Cancer Research*. 2013; 19:6230–6241. [PubMed: 24081976]
- Fiskus W, Verstovsek S, Manshouri T, Smith JE, Peth K, Abhyankar S, McGuirk J, Bhalla KN. Dual PI3K/AKT/mTOR inhibitor BEZ235 synergistically enhances the activity of JAK2 inhibitor against cultured and primary human myeloproliferative neoplasm cells. *Molecular cancer therapeutics*. 2013; 12:577–588. [PubMed: 23445613]
- Harrison C, Kiladjian JJ, Al-Ali HK, Gisslinger H, Waltzman R, Stalbovska V, McQuitty M, Hunter DS, Levy R, Knoops L, et al. JAK inhibition with ruxolitinib versus best available therapy for myelofibrosis. *The New England journal of medicine*. 2012; 366:787–798. [PubMed: 22375970]
- James C, Ugo V, Le Couedic JP, Staerk J, Delhommeau F, Lacout C, Garcon L, Raslova H, Berger R, Bennaceur-Griscelli A, et al. A unique clonal JAK2 mutation leading to constitutive signalling causes polycythaemia vera. *Nature*. 2005; 434:1144–1148. [PubMed: 15793561]
- Klampfl T, Gisslinger H, Harutyunyan AS, Nivarthi H, Rumi E, Milosevic JD, Them NC, Berg T, Gisslinger B, Pietra D, et al. Somatic mutations of calreticulin in myeloproliferative neoplasms. *The New England journal of medicine*. 2013; 369:2379–2390. [PubMed: 24325356]
- Koppikar P, Abdel-Wahab O, Hedvat C, Marubayashi S, Patel J, Goel A, Kucine N, Gardner JR, Combs AP, Vaddi K, et al. Efficacy of the JAK2 inhibitor INCB16562 in a murine model of MPLW515L-induced thrombocytosis and myelofibrosis. *Blood*. 2010; 115:2919–2927. [PubMed: 20154217]
- Koppikar P, Bhagwat N, Kilpivaara O, Manshouri T, Adli M, Hricik T, Liu F, Saunders LM, Mullally A, Abdel-Wahab O, et al. Heterodimeric JAK-STAT activation as a mechanism of persistence to JAK2 inhibitor therapy. *Nature*. 2012; 489:155–159. [PubMed: 22820254]
- Kralovics R, Passamonti F, Buser AS, Teo SS, Tiedt R, Passweg JR, Tichelli A, Cazzola M, Skoda RC. A gain-of-function mutation of JAK2 in myeloproliferative disorders. *The New England journal of medicine*. 2005; 352:1779–1790. [PubMed: 15858187]
- Kubovcakova L, Lundberg P, Grisouard J, Hao-Shen H, Romanet V, Andraos R, Murakami M, Dirnhofer S, Wagner KU, Radimerski T, Skoda RC. Differential effects of hydroxyurea and INC424 on mutant allele burden and myeloproliferative phenotype in a JAK2-V617F polycythemia vera mouse model. *Blood*. 2013; 121:1188–1199. [PubMed: 23264594]
- Levine RL, Wadleigh M, Cools J, Ebert BL, Wernig G, Huntly BJ, Boggon TJ, Wlodarska I, Clark JJ, Moore S, et al. Activating mutation in the tyrosine kinase JAK2 in polycythemia vera, essential thrombocythemia, and myeloid metaplasia with myelofibrosis. *Cancer cell*. 2005; 7:387–397. [PubMed: 15837627]
- Marubayashi S, Koppikar P, Taldone T, Abdel-Wahab O, West N, Bhagwat N, Caldas-Lopes E, Ross KN, Gonen M, Gozman A, et al. HSP90 is a therapeutic target in JAK2-dependent myeloproliferative neoplasms in mice and humans. *The Journal of clinical investigation*. 2010; 120:3578–3593. [PubMed: 20852385]

- Mullally A, Lane SW, Ball B, Megerdichian C, Okabe R, Al-Shahrour F, Paktinat M, Haydu JE, Housman E, Lord AM, et al. Physiological Jak2V617F expression causes a lethal myeloproliferative neoplasm with differential effects on hematopoietic stem and progenitor cells. *Cancer cell*. 2010; 17:584–596. [PubMed: 20541703]
- Nangalia J, Massie CE, Baxter EJ, Nice FL, Gundem G, Wedge DC, Avezov E, Li J, Kollmann K, Kent DG, et al. Somatic CALR mutations in myeloproliferative neoplasms with nonmutated JAK2. *The New England journal of medicine*. 2013; 369:2391–2405. [PubMed: 24325359]
- Pardanani AD, Levine RL, Lasho T, Pikman Y, Mesa RA, Wadleigh M, Steensma DP, Elliott MA, Wolanskyj AP, Hogan WJ, et al. MPL515 mutations in myeloproliferative and other myeloid disorders: a study of 1182 patients. *Blood*. 2006; 108:3472–3476. [PubMed: 16868251]
- Pikman Y, Lee BH, Mercher T, McDowell E, Ebert BL, Gozo M, Cuker A, Wernig G, Moore S, Galinsky I, et al. MPLW515L is a novel somatic activating mutation in myelofibrosis with myeloid metaplasia. *PLoS medicine*. 2006; 3:e270. [PubMed: 16834459]
- Pronk CJ, Rossi DJ, Mansson R, Attema JL, Norddahl GL, Chan CK, Sigvardsson M, Weissman IL, Bryder D. Elucidation of the phenotypic, functional, and molecular topography of a myeloerythroid progenitor cell hierarchy. *Cell stem cell*. 2007; 1:428–442. [PubMed: 18371379]
- Rampal R, Al-Shahrour F, Abdel-Wahab O, Patel JP, Brunel JP, Mermel CH, Bass AJ, Pretz J, Ahn J, Hricik T, et al. Integrated genomic analysis illustrates the central role of JAK-STAT pathway activation in myeloproliferative neoplasm pathogenesis. *Blood*. 2014; 123:e123–133. [PubMed: 24740812]
- Schuringa JJ, Wu K, Morrone G, Moore MA. Enforced activation of STAT5A facilitates the generation of embryonic stem-derived hematopoietic stem cells that contribute to hematopoiesis in vivo. *Stem Cells*. 2004; 22:1191–1204. [PubMed: 15579639]
- Schwaab J, Ernst T, Erben P, Rinke J, Schnittger S, Strobel P, Metzgeroth G, Mossner M, Haferlach T, Cross NC, et al. Activating CBL mutations are associated with a distinct MDS/MPN phenotype. *Annals of hematology*. 2012; 91:1713–1720. [PubMed: 23010802]
- Scott LM, Tong W, Levine RL, Scott MA, Beer PA, Stratton MR, Futreal PA, Erber WN, McMullin MF, Harrison CN, et al. JAK2 exon 12 mutations in polycythemia vera and idiopathic erythrocytosis. *The New England journal of medicine*. 2007; 356:459–468. [PubMed: 17267906]
- Tong W, Zhang J, Lodish HF. Lnk inhibits erythropoiesis and Epo-dependent JAK2 activation and downstream signaling pathways. *Blood*. 2005; 105:4604–4612. [PubMed: 15705783]
- Tyner JW, Bumm TG, Deininger J, Wood L, Aichberger KJ, Loriaux MM, Druker BJ, Burns CJ, Fantino E, Deininger MW. CYT387, a novel JAK2 inhibitor, induces hematologic responses and normalizes inflammatory cytokines in murine myeloproliferative neoplasms. *Blood*. 2010; 115:5232–5240. [PubMed: 20385788]
- Ungureanu D, Wu J, Pekkala T, Niranjani Y, Young C, Jensen ON, Xu CF, Neubert TA, Skoda RC, Hubbard SR, Silvennoinen O. The pseudokinase domain of JAK2 is a dual-specificity protein kinase that negatively regulates cytokine signaling. *Nature structural & molecular biology*. 2011; 18:971–976.
- Vannucchi AM, Antonioli E, Guglielmelli P, Pancrazzi A, Guerini V, Barosi G, Ruggeri M, Specchia G, Lo-Coco F, Delaini F, et al. Characteristics and clinical correlates of MPL 515W>L/K mutation in essential thrombocythemia. *Blood*. 2008; 112:844–847. [PubMed: 18519816]
- Verstovsek S, Mesa RA, Gotlib J, Levy RS, Gupta V, DiPersio JF, Catalano JV, Deininger M, Miller C, Silver RT, et al. A double-blind, placebo-controlled trial of ruxolitinib for myelofibrosis. *The New England journal of medicine*. 2012; 366:799–807. [PubMed: 22375971]
- Verstovsek S, Mesa RA, Gotlib J, Levy RS, Gupta V, DiPersio JF, Catalano JV, Deininger MW, Miller CB, Silver RT, et al. Efficacy, safety and survival with ruxolitinib in patients with myelofibrosis: results of a median 2-year follow-up of COMFORT-I. *Haematologica*. 2013; 98:1865–1871. [PubMed: 24038026]
- Weigert O, Lane AA, Bird L, Kopp N, Chapuy B, van Bodegom D, Toms AV, Marubayashi S, Christie AL, McKeown M, et al. Genetic resistance to JAK2 enzymatic inhibitors is overcome by HSP90 inhibition. *The Journal of experimental medicine*. 2012; 209:259–273. [PubMed: 22271575]

- Zhao R, Xing S, Li Z, Fu X, Li Q, Krantz SB, Zhao ZJ. Identification of an acquired JAK2 mutation in polycythemia vera. *The Journal of biological chemistry*. 2005; 280:22788–22792. [PubMed: 15863514]
- Zhu Z, Aref AR, Cohoon TJ, Barbie TU, Imamura Y, Yang S, Moody SE, Shen RR, Schinzel AC, Thai TC, et al. Inhibition of KRAS-driven tumorigenicity by interruption of an autocrine cytokine circuit. *Cancer discovery*. 2014; 4:452–465. [PubMed: 24444711]

### Significance

Although clinically tested JAK inhibitors provide clinical benefit to MPN patients, molecular responses are not observed in most MPN patients treated with them. We previously demonstrated MPN cells can acquire persistence to type I JAK inhibitors, which bind the active conformation of JAK2 and enable activation of JAK2 *in trans* by other JAK family members. We show that the type II inhibitor CHZ868, which binds JAK2 in the inactive conformation, retains efficacy in type I JAK inhibitor persistent cells. CHZ868 shows increased efficacy in murine models of polycythemia vera and myelofibrosis, including significant reductions in allele burden not observed with first-generation JAK inhibitors. These data demonstrate type II JAK inhibitors can provide improved JAK2 target inhibition, offering increased therapeutic efficacy.

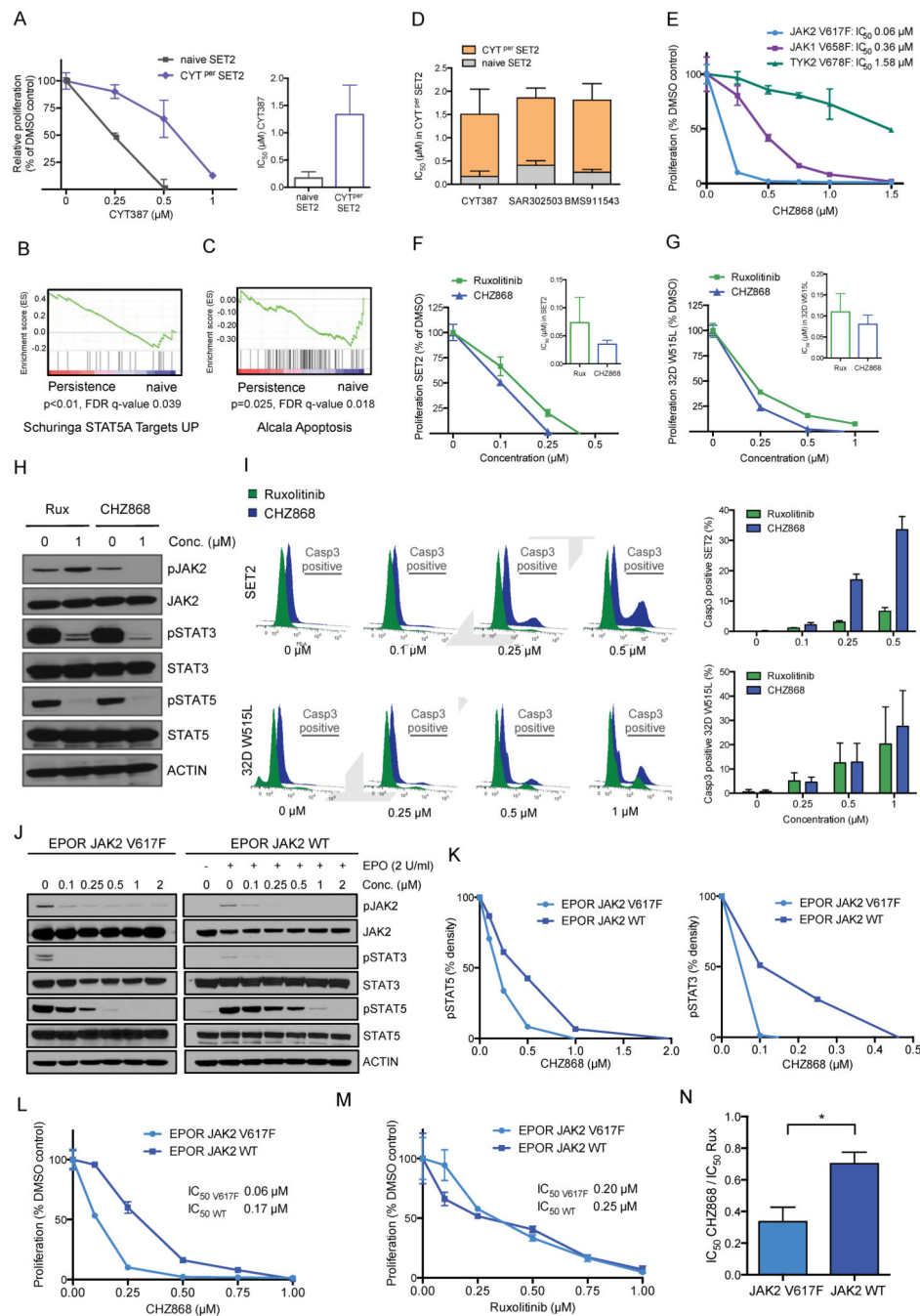


**Figure 1. Type II JAK2 inhibition by CHZ868 in naive MPN cells**

**A.** Proliferation with increasing concentrations of CYT387 ( $\mu\text{M}$ ) relative to proliferation in the presence of DMSO as control is shown for naive SET2 cells and for SET2 cells chronically cultured in the presence of CYT387 (CYT<sup>per</sup> SET2) (left panel).  $\text{IC}_{50}$  values for CYT387 are indicated in naive SET2 and in CYT<sup>per</sup> SET2 (right panel). Data of both panels are indicated as mean  $\pm$  SEM. **B.** The STAT5 gene expression signature as described by Schuringa et al (Schuringa et al., 2004) is tested for enrichment by gene set enrichment analysis (GSEA) in type I JAK inhibitor persistent cells vs. naive SET2 cells. **C.** The



apoptosis gene expression signature as described by Alcala et al (Alcala et al., 2008) is tested for enrichment by GSEA in type I JAK inhibitor persistent cells vs. naive SET2 cells. **D.** The  $IC_{50}$  values for CYT387, SAR302503 and BMS911543 in SET2 cells chronically cultured in the presence of CYT387 (CYT<sup>per</sup> SET2) are shown as mean  $\pm$  SEM along with the respective  $IC_{50}$  values in naive SET2 cells. **E.** The proliferation of Ba/F3 cells stably expressing JAK2 V617F, JAK1 V658F or TYK2 V678F in the presence of increasing concentrations of CHZ868 ( $\mu$ M) is shown relative to proliferation in the presence of DMSO. Data are represented as mean  $\pm$  SEM. Indicated  $IC_{50}$  values represent the mean of two independent experiments performed in triplicate. **F.** Proliferation of JAK2V617F SET2 cells in increasing concentrations of inhibitor vs. DMSO is shown for CHZ868 and for ruxolitinib.  $IC_{50}$  values of CHZ868 and ruxolitinib in SET2 cells are indicated in the inset. All data are represented as mean  $\pm$  SEM. **G.** Proliferation of 32D cells expressing MPLW515L, in increasing concentrations of inhibitor vs. DMSO is shown for CHZ868 and for ruxolitinib.  $IC_{50}$  values of CHZ868 and ruxolitinib in 32D MPLW515L cells are indicated in the inset. All data are represented as mean  $\pm$  SEM. **H.** The effect of CHZ868 on phosphorylation of JAK2, STAT3 and STAT5 in SET2 cells is shown in comparison to ruxolitinib. **I.** Induction of apoptosis by increasing concentrations of CHZ868 as compared to ruxolitinib is shown in JAK2V617F SET2 cells and in 32D MPLW515L cells as the proportion of Caspase-3 positive cells by representative flow cytometry histograms (left panel) and by bar graphs indicating data as mean  $\pm$  SEM (right panel). **J.** The effect of increasing concentrations of CHZ868 on the phosphorylation of JAK2, STAT3 and STAT5 is assessed in Ba/F3 cells stably expressing EPOR JAK2 V617F as compared to EPOR JAK2 WT Ba/F3 cells. **K.** Densitometry of pSTAT5 and pSTAT3 Western blot bands displayed in Fig 1J. **L.** Proliferation of EPOR JAK2 V617F Ba/F3 cells in the presence of increasing concentrations CHZ868 ( $\mu$ M) relative to proliferation in presence of DMSO is compared to the proliferation of EPOR JAK2 WT Ba/F3 cells. Data are represented as mean  $\pm$  SEM.  $IC_{50}$  values represent the mean of 2 independent experiments performed in triplicate. **M.** Proliferation of EPOR JAK2 V617F Ba/F3 cells in the presence of increasing concentrations ruxolitinib ( $\mu$ M) relative to proliferation in presence of DMSO is compared to the proliferation of EPOR JAK2 WT Ba/F3 cells. Data are represented as mean  $\pm$  SEM.  $IC_{50}$  values represent the mean of 2 independent experiments performed in triplicate. **N.** The ratio of  $IC_{50}$  for CHZ868 to  $IC_{50}$  for ruxolitinib is compared for EPOR JAK2 V617F and EPOR JAK2 WT Ba/F3 cells. Data are represented as mean  $\pm$  SEM, \* $p < 0.05$ . See also Figure S1.

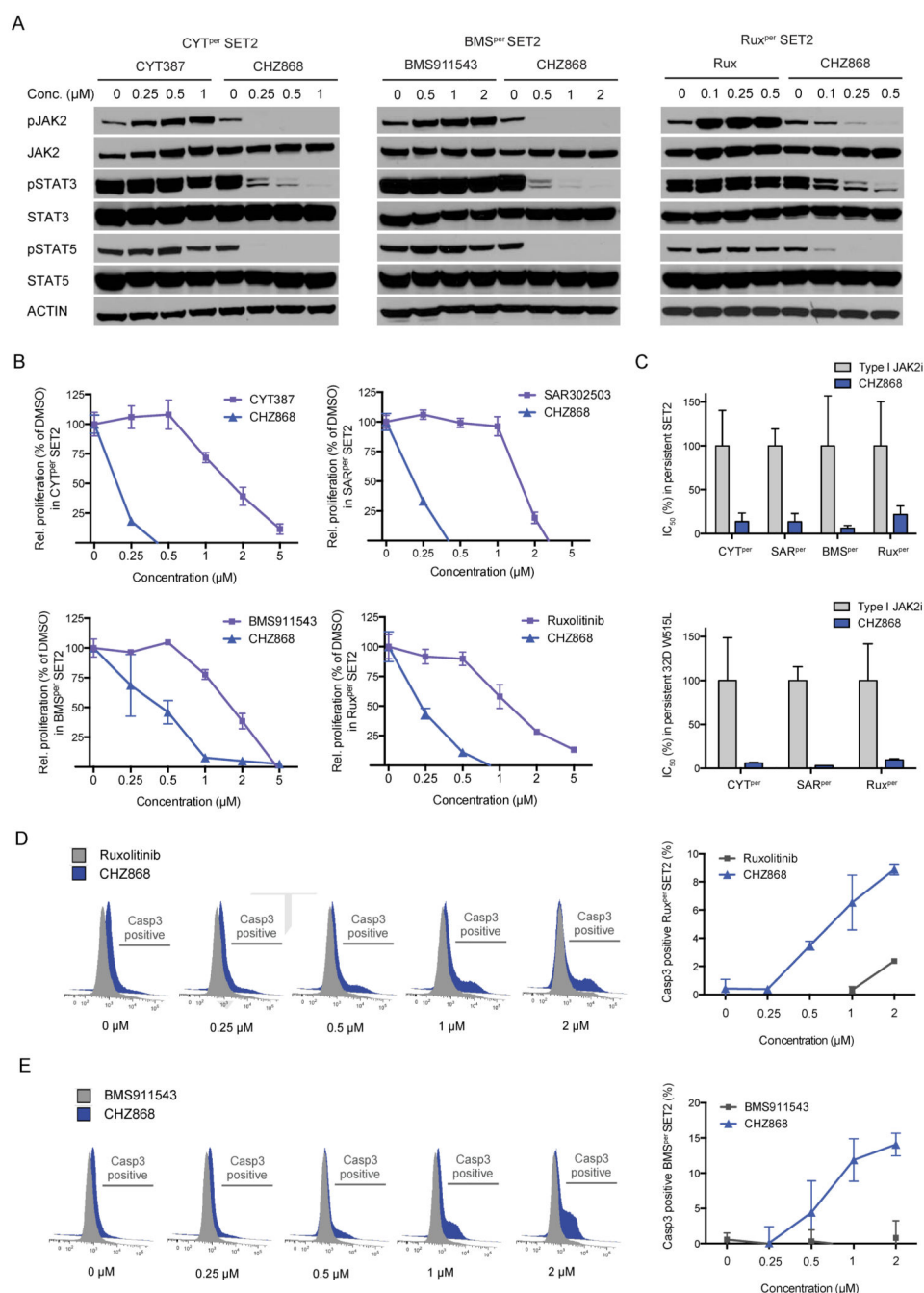


**Figure 2. Type II JAK2 inhibition by CHZ868 in persistence to type I JAK inhibitors**

**A.** Effect of 4 hr incubation with increasing concentrations of CHZ868 or with the respective type I JAK inhibitor on phosphorylation of JAK2, STAT3 and STAT5 in CYT387 (CYT<sup>per</sup>), BMS911543 (BMS<sup>per</sup>) or ruxolitinib (Rux<sup>per</sup>) persistent SET2 cells. **B.** Proliferation of CYT387 (CYT<sup>per</sup>), SAR302503 (SAR<sup>per</sup>), BMS911543 (BMS<sup>per</sup>) or ruxolitinib (Rux<sup>per</sup>) persistent SET2 cells upon increasing concentrations of the respective type I JAK inhibitor or CHZ868 relative to proliferation in the presence of DMSO. All data are represented as mean  $\pm$  SEM. **C.** IC<sub>50</sub> values for CHZ868 in CYT387, SAR302503,

BMS911543 and ruxolitinib persistent *JAK2V617F* SET2 and *MPLW515L* 32D cells is shown relative to the IC50 values of the respective type I JAK inhibitors. Data are represented as mean  $\pm$  SEM. **D.** Induction of apoptosis with increasing concentrations of CHZ868 or ruxolitinib in Rux<sup>per</sup> SET2 cells is shown by the proportion of Caspase-3 positive cells in representative flow cytometry histograms (left panel) and as mean  $\pm$  SEM (right panel). **E.** Induction of apoptosis with increasing concentrations of CHZ868 or BMS911543 in BMS<sup>per</sup> SET2 cells is shown in representative flow cytometry histograms (left panel) and as mean  $\pm$  SEM (right panel). See also Figure S2.

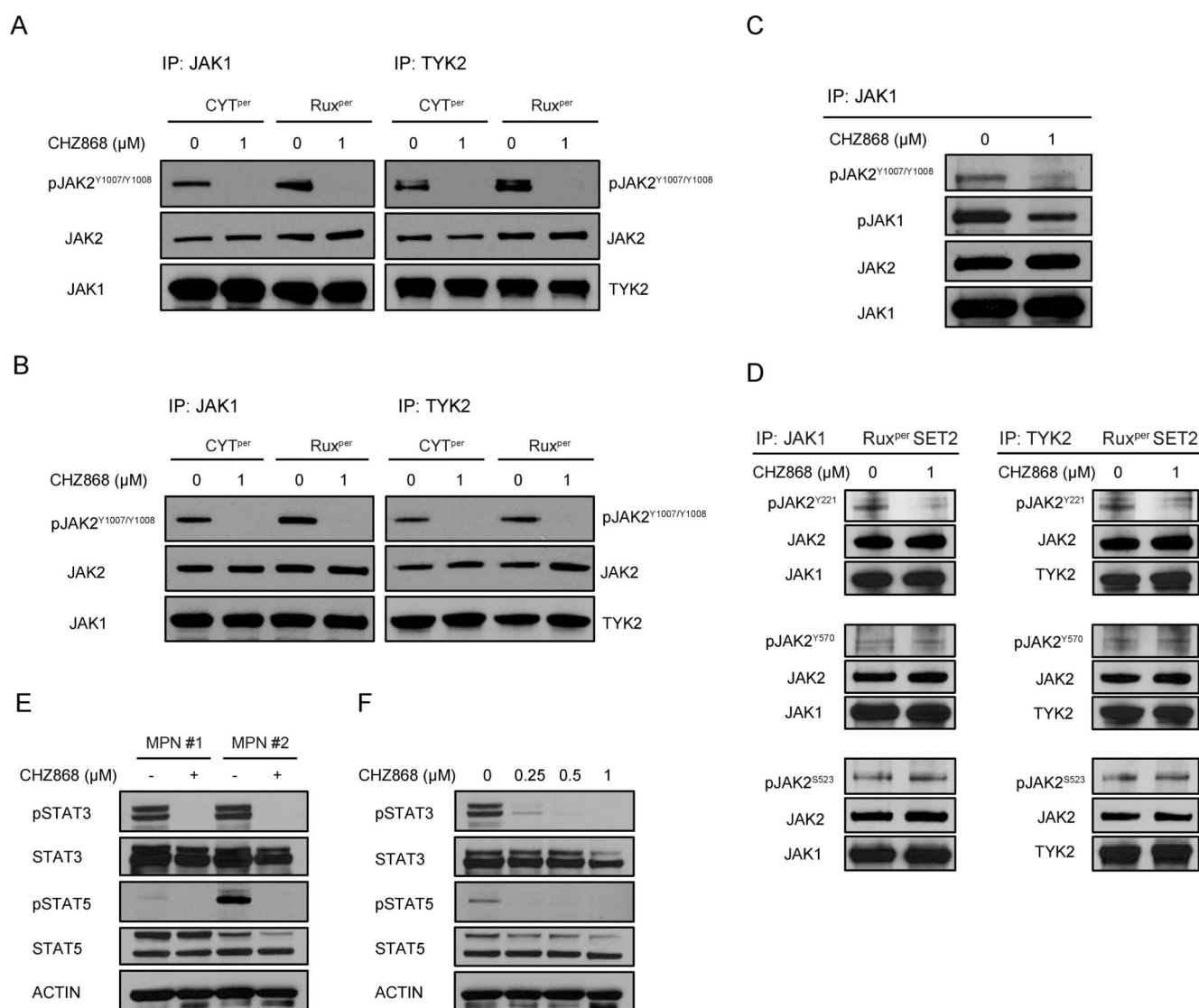


**Figure 3. Effect of type II JAK2 inhibition with CHZ868 on transphosphorylation of JAK2 in heterodimers**

**A.** The phosphorylation at Y1007/Y1008 of JAK2 co-immunoprecipitated with JAK1 (left panel) or TYK2 (right panel) is shown after 4 hr incubation of CYT387 (CYT<sup>per</sup>) and ruxolitinib (Rux<sup>per</sup>) persistent SET2 cells with CHZ868 or DMSO as control. **B.** The phosphorylation at Y1007/Y1008 of JAK2 is also assessed after 20 hr incubation with CHZ868 or DMSO as control. **C.** Phosphorylation of JAK2 at Y1007/Y1008 and phosphorylation of JAK1 are assessed in γ2A cells deficient of endogenous JAK2 and stably expressing constitutively active JAK1 V658F and kinase dead JAK2 K882E after 4 hr exposure to CHZ868. **D.** Phosphorylation at Y221 of JAK2 (top row) co-immunoprecipitated with JAK1 (left panel) or TYK2 (right panel) as well as phosphorylation at Y570 (middle row) and at S523 (bottom row) are shown after 4 hr incubation with CHZ868. **E.** Phosphorylation of STAT3 and STAT5 in freshly isolated peripheral blood mononuclear cells from MPN patients on long-term ruxolitinib treatment is

assessed after 16 hr ex vivo exposure with CHZ868. **F.** STAT3 and STAT5 phosphorylation in freshly isolated peripheral blood mononuclear cells from a chronically ruxolitinib treated MPN patient is also assessed after 16 hr ex vivo exposure with increasing concentrations of CHZ868. See also Figure S3.

Author Manuscript

Author Manuscript

Author Manuscript

Author Manuscript



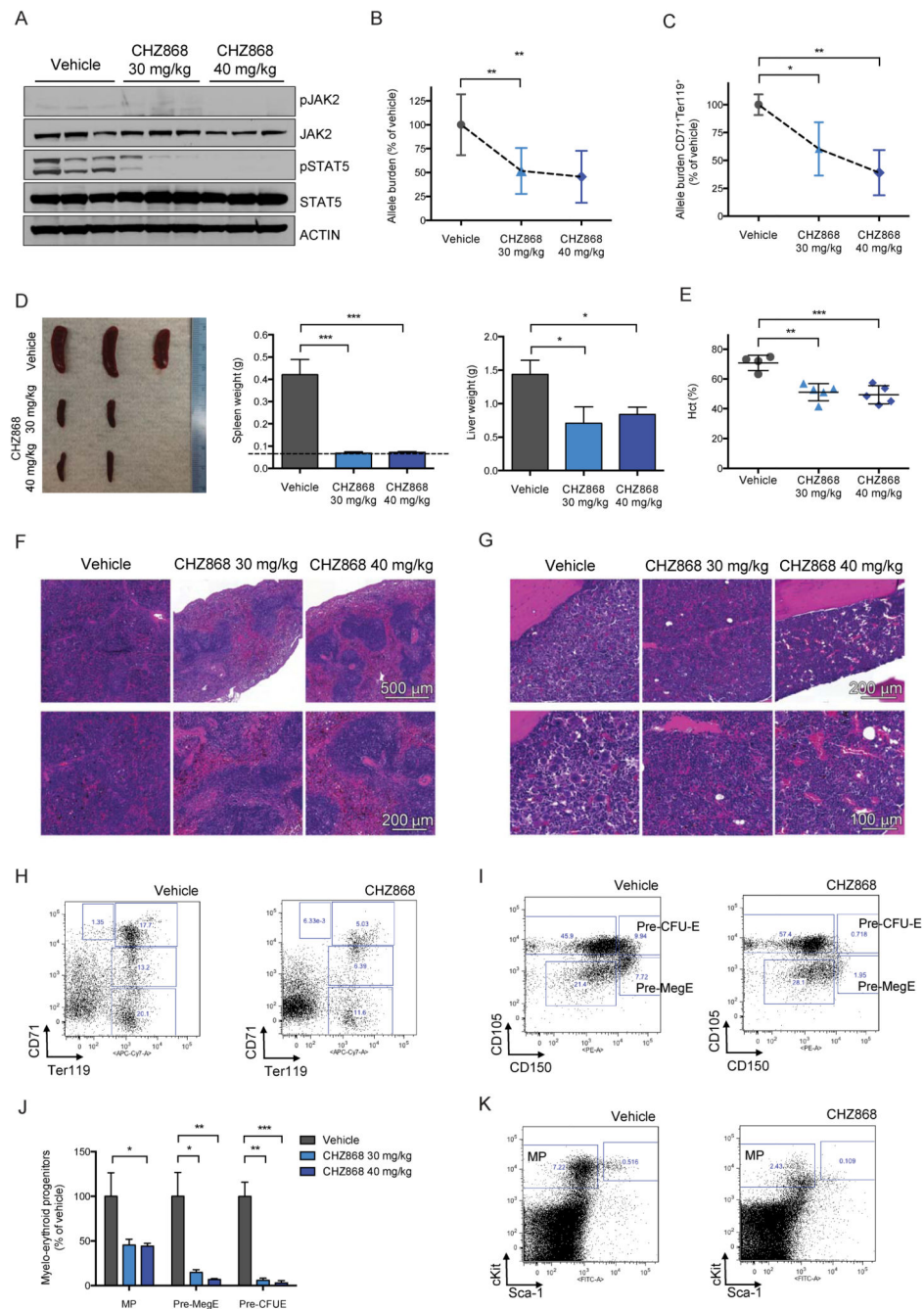


**Figure 4. Type II JAK2 inhibition by CHZ868 in vivo in the conditional *Jak2V617F* knock-in model of polycythemia vera**

**A.** JAK2 and STAT5 phosphorylation are assessed after 14 days of treatment with 30 mg/kg and 40 mg/kg CHZ868 in the conditional *Jak2V617F* knock-in model of PV. **B.** Allele burden as reflected by CD45.2 donor chimerism in primary recipients of *Jak2V617F* knock-in bone marrow is shown after 14 days of treatment with 30 mg/kg and 40 mg/kg CHZ868 relative to vehicle-treated mice (n=6-7 mice/group, data represented as mean  $\pm$  SEM, \*\*p<0.01 versus vehicle group). **C.** Mutant allele burden is at 60.4% and 39.0% in recipients

of *Jak2V617F* knock-in bone marrow treated with 30 and 40 mg/kg CHZ868 relative to vehicle-treated mice specifically in the CD71<sup>+</sup>Ter119<sup>+</sup> erythroid progenitor compartment. Data are represented as mean ± SEM. (\*p<0.05, \*\*p<0.01 versus vehicle group). **D.** Spleen size and weight as well as liver weight at 14 days of treatment with CHZ868 30 mg/kg or 40 mg/kg. The dashed line indicates the spleen weight of age-matched control mice. Data are represented as mean ± SEM (\*p<0.05, \*\*\*p<0.001 versus vehicle group). **E.** Hematocrit (Hct) at 14 days of treatment with CHZ868 30 mg/kg or 40 mg/kg. Data are represented as mean ± SEM (\*\*p<0.01 or \*\*\*p<0.001 versus vehicle group). **F.** Splenic architecture and the extent of myelo-erythroid infiltration of the spleen is shown in vehicle-treated as compared to CHZ868-treated animals. **G.** Bone marrow histology with a particular focus on megakaryocyte number is shown in vehicle- and CHZ868-treated mice. **H.** The CD71<sup>+</sup>Ter119<sup>+</sup> proerythroblast population in vehicle- and CHZ868-treated animals is illustrated by representative flow cytometry plots (p=0.036 and p=0.015 at 30 and 40 mg/kg CHZ868 versus vehicle group, respectively). **I.** Lin<sup>-</sup> cKit<sup>high</sup>CD41<sup>-</sup>FcgR<sup>-</sup>CD150<sup>+</sup>CD105<sup>+</sup> committed erythroid progenitors (Pre-CFUE) and Lin<sup>-</sup> cKit<sup>high</sup>CD41<sup>-</sup>FcgR<sup>-</sup>CD150<sup>+</sup>CD105<sup>-</sup> bipotential megakaryocyte-erythroid progenitors (Pre-MegE) are assessed as described (Mullally et al., 2010; Pronk et al., 2007) after treatment with 30 and 40 mg/kg CHZ868 (Pre-CFUE p<0.01 and p<0.001; Pre-MegE p=0.02 and p<0.01 versus vehicle group, respectively), and representative flow cytometry plots are shown. **J.** Myeloerythroid progenitor frequencies including multipotent myeloid progenitors (MP), bipotential megakaryocyte-erythroid progenitors (Pre-MegE) and committed erythroid progenitors (Pre-CFUE) after treatment with CHZ868 30 mg/kg and 40 mg/kg for 14 days are indicated relative to vehicle-treated animals. Data are represented as mean ± SEM (\*p<0.05, \*\*p<0.01, \*\*\*p<0.001 versus vehicle group). **K.** Representative flow cytometry plots are shown for Lin<sup>-</sup>Sca1<sup>-</sup>Kit<sup>+</sup> multipotent myeloid progenitors in the presence and absence of CHZ868 treatment (p=0.02). See also Figure S4.

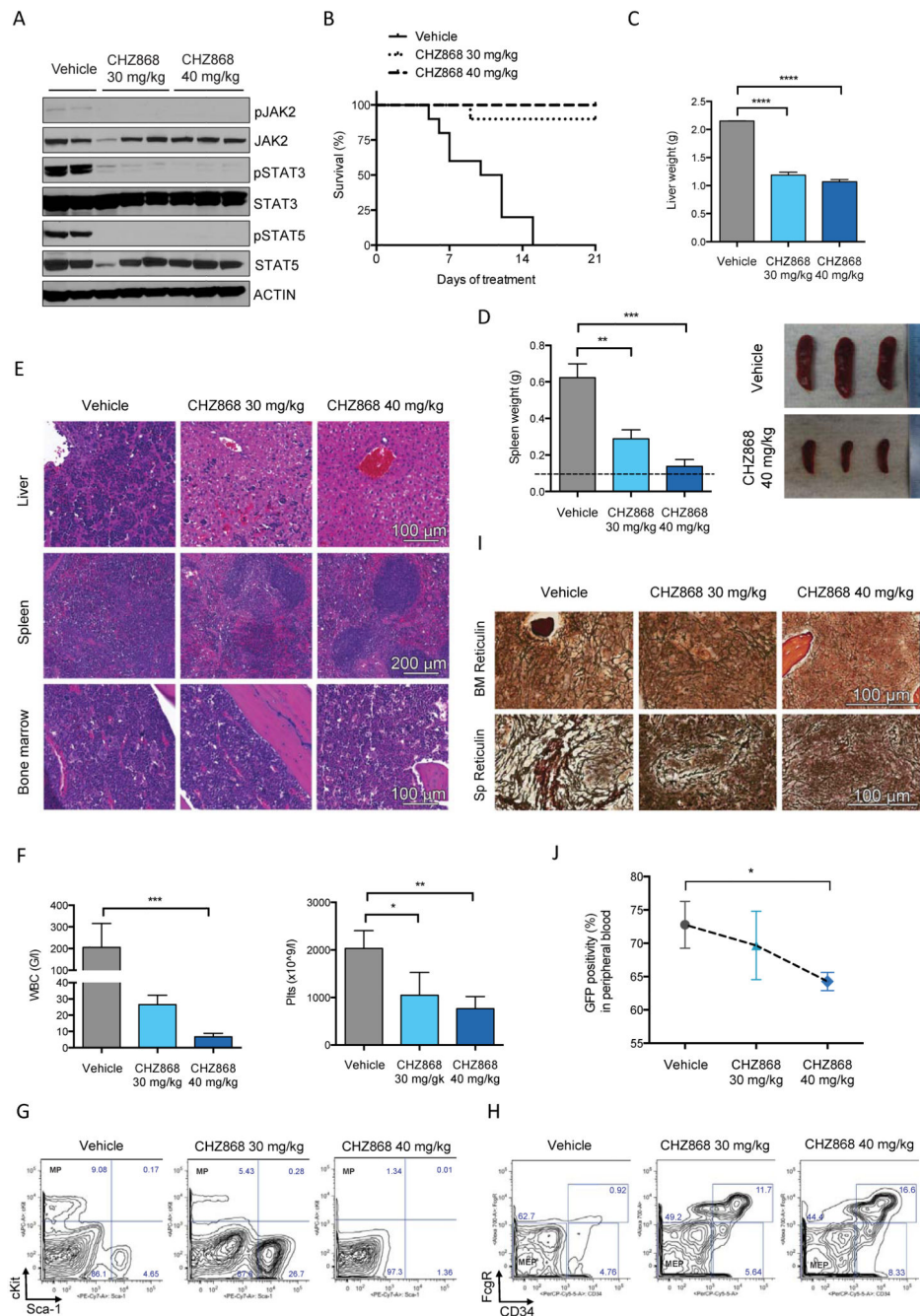


**Figure 5. Type II JAK2 inhibition by CHZ868 in vivo in the MPLW515L model of myelofibrosis**  
**A.** Phosphorylation of JAK2, STAT3 and STAT5 is evaluated after 3 doses of CHZ868 at 30 mg/kg or 40 mg/kg in the MPLW515L model. **B.** Survival in the MPLW515L model of myelofibrosis upon long-term treatment with CHZ868 ( $p < 0.0001$ , 10-11 mice/arm). **C.** Liver weight in animals treated for 10 days with CHZ868 at 30 mg/kg or 40 mg/kg vs. vehicle treatment. Data are represented as mean  $\pm$  SEM (\*\*\*\* $p < 0.0001$  versus vehicle group). **D.** Spleen weight (left panel) and size (right panel) upon 10 days treatment with CHZ868 30 mg/kg or 40 mg/kg vs. vehicle-treated mice. The dashed line indicates spleen

weight in age-matched controls. Spleen weights are represented as mean  $\pm$  SEM (\*\* $p < 0.01$ , \*\*\* $p < 0.001$  versus vehicle group). **E.** The extent of extramedullary hematopoiesis in the liver (top row) and myeloerythroid infiltration of the spleen (middle row) as well as of megakaryocytic hyperplasia of the bone marrow (bottom row) are shown after 10 days of treatment with CHZ868 30 mg/kg or 40 mg/kg vs. vehicle-treatment. **F.** Peripheral blood white blood cell (WBC) and platelet (Plts) counts are indicated for CHZ868- and vehicle-treated *MPLW515L* mice. Data are represented as mean  $\pm$  SEM (\* $p < 0.05$ , \*\* $p < 0.01$ , \*\*\* $p < 0.001$  versus vehicle group). **G.** Lin<sup>-</sup>Sca1<sup>-</sup>Kit<sup>+</sup> multipotent myeloid progenitors (MP) of CHZ868- and vehicle-treated *MPLW515L* mice are shown in representative flow cytometry plots. **H.** The impact of CHZ868 treatment on Lin<sup>-</sup>Sca1<sup>-</sup>Kit<sup>+</sup>FcgR<sup>-</sup>CD34<sup>-</sup> megakaryocytic-erythroid progenitors (MEP) in the *MPLW515L* model is also assessed. **I.** The impact of 10 days CHZ868 treatment on reticulin fibrosis which represents a hallmark of the *MPLW515L* model of myelofibrosis, is assessed by silver staining of bone marrow (BM, top row) and spleen (Sp, bottom row). **J.** Mutant allele burden as reflected by the percentage of GFP<sup>+</sup> cells in peripheral blood is shown at 10 days of treatment with CHZ868 40 mg/kg. Data are represented as mean  $\pm$  SEM (\* $p < 0.05$  versus vehicle group). See also Figure S5.

Table 1

Cross-persistence to type I JAK inhibitors<sup>a</sup> (Proliferation assay IC<sub>50</sub>, nM)

JAK inhibitor	IC <sub>50</sub> naïve	IC <sub>50</sub> Rux <sup>per</sup>	IC <sub>50</sub> CYT387 <sup>per</sup>	IC <sub>50</sub> SAR302503 <sup>per</sup>	IC <sub>50</sub> BMS911543 <sup>per</sup>
Ruxolitinib	0.07	0.90	0.47	0.82	1.0
CYT387	0.17	4.2	1.8	1.7	3.0
SAR302503	0.41	2.3	1.5	1.6	1.3
BMS911543	0.26	6.5	1.6	1.9	3.4

<sup>a</sup>Indicated IC<sub>50</sub>s are derived from experiments in SET2 cells.